

NANOSTRUCTURES

PACS numbers: 79.20.Eb; 75.75.Fk; 78.67.Bf; 52.38.Mf; 81.16.–c
DOI: 10.1070/QE2012v042n02ABEH014779

Evolution of the distribution function of Au nanoparticles in a liquid under the action of laser radiation

N.A. Kirichenko, I.A. Sukhov, G.A. Shafeev, M.E. Shcherbina

Abstract. **Fragmentation of nanoparticles in a liquid under the action of pulsed laser heating is studied theoretically and experimentally. Fragmentation is simulated by solving the kinetic equation for the nanoparticles size distribution function, taking into account the temperature dependence of the thermophysical parameters of the medium. It is shown that fragmentation occurs after separation of smaller fragments from a molten nanoparticle. The simulation results are in good agreement with experimental data obtained in the fragmentation of gold nanoparticles irradiated in water by a copper vapour laser with a peak radiation intensity of about 10^6 W cm^{-2}.**

Keywords: *nanoparticles, colloids, laser ablation of metals, plasmon resonance, fragmentation.*

1. Introduction

Laser ablation of solids in liquids is one of the methods for obtaining nanoparticles. In this process, a solid target immersed in a liquid is subjected to laser irradiation with an energy density on the target surface above the melting threshold. The melt layer at the target surface is dispersed into the surrounding liquid by the recoil vapour pressure. Nanoparticles produced in this way solidify and remain in the liquid, forming a colloidal solution. Under continuing laser irradiation of the target, the produced nanoparticles may reenter the laser beam. Typically, interaction with laser radiation leads to a change in the nanoparticle size – so-called fragmentation. By irradiating a colloidal solution, the nanoparticle size distribution function is shifted to lower values. This effect was observed in the earliest work on laser generation of nanoparticles in liquids [1–3].

It was found that the rate of fragmentation is sensitive to the wavelength of laser radiation [4]. This dependence may be due to absorption of laser radiation by individual nanoparticles through the plasmon resonance of electrons they contain. The wavelength dependence of the fragmentation efficiency of nanoparticles is convincingly demonstrated by Akman et al. [5], who studied experimentally fragmentation of silver nanoparticles irradiated by the first (800 nm) and second (400 nm) harmonics of a Ti:sapphire femtosecond laser. The frequency of the second harmonic of this laser is in good agreement with the plasmon resonance of silver nanoparticles in water (near 400 nm), which results in greater efficiency of absorption of this radiation by nanoparticles. A significant difference between medium-sized nanoparticles of gold and silver upon ablation of the corresponding targets by 800-nm femtosecond light was interpreted as the result of conversion of laser radiation frequency on the nanoparticles to the second harmonic, which is strongly absorbed by the silver nanoparticles [6]. Interaction of femtosecond laser radiation with liquids leads to the generation of a broadband continuum in the medium: If the laser wavelength is far from the plasmon resonance of the generated nanoparticles, the particles can absorb broadband radiation and undergo fragmentation.

Regardless of the laser pulse duration, fragmentation of individual nanoparticles in the laser beam takes place against a background of phase transitions both in the particle and in the surrounding liquid. The liquid surrounding the particle evaporates, forming a vapour-gas cavity. In this case, the medium in this cavity may be in the supercritical region of parameters. Generally speaking, the material of the particle can evaporate into the cavity, and fragmentation can result from evaporation and subsequent condensation in a smaller particle, as well as from viscous interaction of a molten nanoparticle with a dense medium. To reveal the mechanism of fragmentation of nanoparticles in liquids in intense laser beams, experimental data are needed on the evolution of the nanoparticle size distribution function upon the interaction of a laser beam with an ensemble of nanoparticles. In addition, simulation of fragmentation and comparison of theoretical results with experimental data will also allow the most likely scenario of laser fragmentation of the nanoparticles to be established.

The aim of this paper is to study experimentally and theoretically fragmentation of gold nanoparticles in water under the action of visible pulsed laser radiation, whose wavelength is located near the peak of plasmon resonance of the particles. Simulation is performed by solving numerically the kinetic equation for the nanoparticle size distribution function, taking into account the temperature dependence of the thermophysical constants of the medium surrounding the particle.

2. Experimental

A colloidal solution of gold nanoparticles was produced by laser ablation of a gold target in water. A detailed description of the experiment is given in [7, 8]. We used a copper vapour laser with a wavelength of 510.6 and 578.2 nm, pulse repetition rate of 15 kHz, a pulse duration of 20 ns and a peak radi-

N.A. Kirichenko, I.A. Sukhov, G.A. Shafeev, M.E. Shcherbina Wave Research Center, A.M. Prokhorov General Physics Institute, Russian Academy of Sciences, ul. Vavilova 38, 119991 Moscow, Russia; e-mail: kir@kapella.gpi.ru, shafeev@kapella.gpi.ru

Received 28 November 2011
Kvantovaya Elektronika **42** (2) 175–180 (2012)
Translated by I.A. Ulitkin

ation intensity of about 4×10^8 W cm^{-2} at the target surface. The average total laser power at two wavelengths was 4 W. The ratio of the average laser power at wavelengths of 510.6 and 578.2 nm was 3 : 2.

The typical time of the colloidal solution production was a few minutes. The resulting solution (1 – 2 mL) was placed in a cylindrical cell with a window transparent for the laser radiation and was irradiated by a copper vapour laser (without the target). As a result, nanoparticles of the colloidal solution were fragmented, the total mass of particles in the solution remaining the same.

The resulting nanoparticles hardly absorbed radiation at a wavelength of 578.2 nm, so the estimates of the intensity took into account only absorption at $\lambda = 510.6$ nm. In the experiments we varied the time of the solution exposure and the diameter of the laser beam (which determines the peak laser power in the colloid solution) at the entrance to the cell.

The nanoparticle size distribution function was measured by using a CPS DC2400 disk centrifuge, whose operation is based on the principles of differential sedimentation analysis. Nanoparticles were placed in a preliminary prepared sucrose solution with a density gradient and were allowed to settle at different rates under the action of centrifugal force on the inner wall of a transparent rotating disk. Near the edge of the disk we measured absorption at a wavelength of 430 nm. The time of sedimentation was automatically recalculated to the particle size by using the Stokes theory, and absorption – to the particle concentration by using the Mie theory. Preliminary, we tested the performance of the centrifuge using the nanoparticles of size down to 5 nm. For smaller particle sizes the time of sedimentation amounted to many hours, and the measurement accuracy decreased.

The absorption spectra of the samples were analysed using an Ocean Optics fibre spectrometer in the wavelength range from 250 to 800 nm.

3. Experimental results

A typical size distribution function of nanoparticles obtained immediately after irradiation of a gold target in water is presented in Fig. 1. The figure shows that there is a maximum, whose position depends on the conditions of the target irradiation.

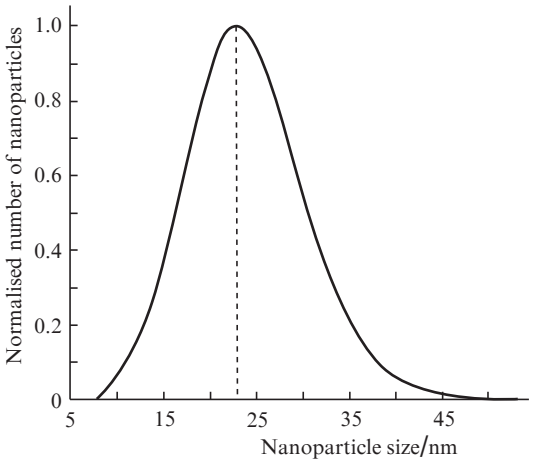

Figure 1. Typical nanoparticle size distribution function obtained by laser ablation of a gold target in water. The maximum of the particle size distribution corresponds to ~23 nm, the FWHM of the distribution function is ~14 nm.

Note that in some experiments, the initial distribution function along with a peak around 20 – 30 nm can exhibit a second peak in the region of small sizes. This is due to the fact that the processes of formation and fragmentation of nanoparticles during the solution preparation were not sufficiently separated. At a high concentration of the particles formed, they fall into the laser beam above the target and become fragmented.

As a result of laser exposure of the colloidal solution (in the absence of the target), the nanoparticle size distribution may differ significantly from the initial one. In particular, there is a shift of the main maximum of the distribution to smaller sizes, as well as an emergence of a new (narrower) peak corresponding to the small particle sizes (Figs 2, 3). With increasing radiation intensity and exposure time remaining constant, the main peak is shifted to the region of smaller sizes. Under sufficiently long irradiation of the colloidal solution and/or at a high peak intensity of the laser beam at the entrance to the solution, the peak of the distribution, referring to the large size particles, completely disappears, and there is only a peak in the region of small sizes. The observed intensity of the latter decreases as laser irradiation continues, because fragmented nanoparticles become increasingly small (subnanometre-sized), and their sizes are already out of the sensitivity of the centrifuge. In this experiment, significant changes in the distribution function have occurred during a few minutes of laser exposure.

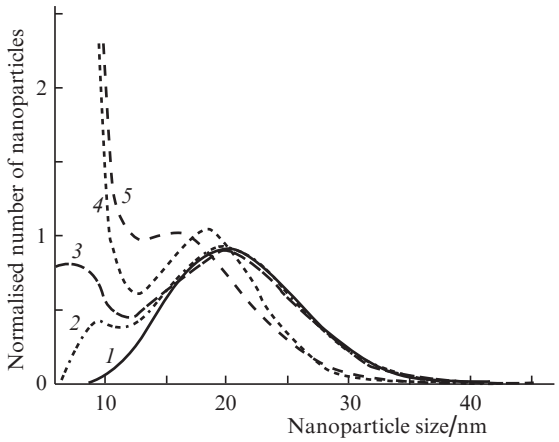

Figure 2. Evolution of the normalised distribution function of nanoparticles by their mass upon fragmentation of the colloidal solution of gold nanoparticles by laser radiation of various intensities I (exposure time of 5 min): (*1*) initial distribution; (*2*) $I = 2.5 \times 10^5$ W cm^{-2}; (*3*) $I = 1.0 \times 10^6$ W cm^{-2}; (*4*) $I = 4.0 \times 10^6$ W cm^{-2}; (*5*) $I = 2.5 \times 10^7$ W cm^{-2}.

In the absorption curve (*1*) (Fig. 4), we may see a 'shoulder' in the long-wavelength region, which is due to the presence of elongated and large particles. One can see that as the irradiation continues, these particles become smaller in number [curves (*2*) and (*3*)].

4. Mathematical model

We assume the particle to be spherically symmetric. We introduce a particle size distribution function $n(r, t)$ such that the quantity $n(r, t)\mathrm{d}r$ represents the number of particles of radius

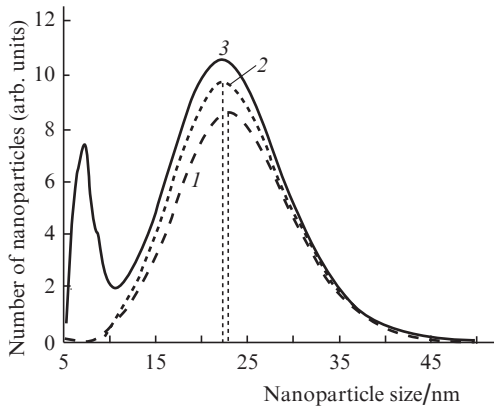

Figure 3. Evolution of the distribution function upon fragmentation of the colloidal solution of gold nanoparticles (the intensity of radiation at the entrance to the colloidal solution is 10^6 W cm^{-2}): (*1*) initial distribution; (*2*) irradiation time t = 1 min; (*3*) t = 10 min.

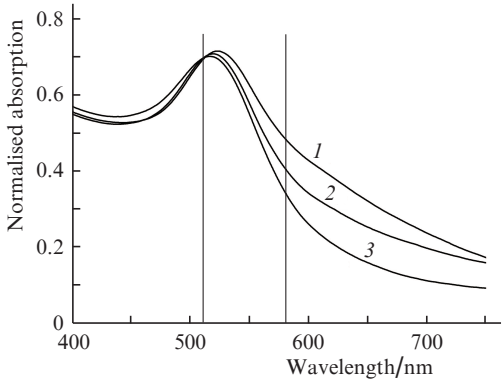

Figure 4. Evolution of the absorption spectrum of the colloidal solution of gold nanoparticles under laser irradiation of the colloidal solution (the intensity is 4×10^8 W cm^{-2}): (*1*) initial distribution; (*2*) irradiation time t = 10 min; (*3*) t = 20 min. The vertical lines indicate the wavelengths of a copper vapour laser.

r in the solution at an instant t. Because the total mass M of particles in the solution is constant, the law of conservation of mass

$$M = \int_0^\infty \rho \frac{4\pi r^3}{3} n(r,t)\mathrm{d}r \qquad (1)$$

should be fulfilled, where ρ is the density of the particle.

In the experiments we measured the quantity $m(r,t)$, whose meaning is that $m(r,t)\mathrm{d}r$ is the total mass of particles with radii in the range of $(r, r+\mathrm{d}r)$. It is obvious that $n(r,t) = m(r,t)/(\rho v(r))$, where $v(r) = (4\pi/3)r^3$ is the volume of the particle.

First, we note that the initial particle distribution function (Fig. 1) is satisfactorily described by the formula

$$n_0(r) = n_0(r,0) = A\exp[-v(r)/v_0],$$
$$m_0(r) = A\rho\exp[-v(r)/v_0]\, v(r), \qquad (2)$$

where A and v_0 are the constants. Using the data from Figs 1 and 2, we can find

$$v_0 \approx 2.5 \times 10^3 \text{ nm}^3, \quad r_0 = (3v_0/4\pi)^{1/3} \approx 8.5 \text{ nm}.$$

Equation (2) is formally similar to the known law of evaporation, in which the density of the flux of evaporated particles is

$$j \sim \exp[(-mL_1/(k_\mathrm{B}T)] = \exp(-v/v_1), \quad v_1 = k_\mathrm{B}T/(\rho L_1), \qquad (3)$$

where L_1 is the effective specific heat of evaporation; m is the mass of a particle (atom); $v = m/\rho$ is the volume of the separating fragment. In particular, for gold (L_1 = 1.73 kJ g^{-1}, ρ = 19.3 g cm^{-3}) $v_1 \approx 1.2 \times 10^{-3}$ nm^3 (v_1 is estimated at temperature $T \sim 3000$ K). Note that the characteristic linear size associated with v_1 is $r_1 = (3v_1/4\pi)^{1/3} \approx 0.14$ nm, i.e., of the order of the size of an atom of gold.

Thus, the numerical values of v_0 and v_1 vary greatly. This indicates a significant difference between the mechanisms of ablation in vacuum (gas) and in a liquid. We can assume that in a liquid ablation is stimulated by the movement of a dense medium, leading to the removal of not only small but also relatively large fragments of material from the target surface. This may be due to a decrease in the surface tension of the metal surface with increasing temperature and ambient pressure. In this case, of course, the probability of separation of a fragment from the target decreases with increasing its size. We note in this connection that due to the smallness of the values of v_1 in (3), only monatomic particles are present in the products of evaporation.

After subsequent irradiation of the colloidal solution the distribution function changes, as is evident from Fig. 2. The particles in the liquid can experience such processes as splitting (fragmentation) and sticking.

Colliding, the nanoparticles can agglomerate and form larger particles. In this case, there should form the additional maxima in the distribution function in the region of sizes greater than the characteristic value, which corresponds to the maximum of the initial distribution $r_{\mathrm{m}0}$. This process plays a significant role if the particle density is sufficiently high. The results of experiments show that in our conditions such maxima do not appear. In addition, the estimates show that for the particle density in the solution, which was achieved in the experiments, the collision frequency is too small to lead to a significant increase in the number of particles with sizes $r > r_{\mathrm{m}0}$.

Another process is the fragmentation of particles. Earlier the authors of [7, 8] theoretically considered the situation where the particles are most likely to be divided into two halves, like a liquid droplet. It was assumed that the particle undergoes a transition to a liquid state, and vapour pressure fluctuations lead to its fragmentation. Such a process should have been accompanied by the appearance of a series of additional maxima in the distribution function at sizes $r \sim 2^{-1/3}r_{\mathrm{m}0}$, $2^{-2/3}r_{\mathrm{m}0}, \ldots$. However, in experiments we failed to observe such intermediate maxima. Therefore, we can assume that the particles fragmented according to the law, similar to (2), i.e., through separation of small clusters, and not through the atomic evaporation.

With the above-said in mind, let us consider the evolution of the distribution function of nanoparticles, taking into account only the processes of fragmentation. We write the kinetic equation for the particle number $n(r,t)$ in the form:

$$\frac{\partial n(r,t)}{\partial t} = \frac{1}{r}\int_r^\infty B(x,r)n(x,t)\frac{\mathrm{d}x}{x^2} - \frac{1}{r^5}\int_0^r B(r,x)n(r,t)x^2\mathrm{d}x. \qquad (4)$$

The first term in the right-hand side of equation (4) describes the increase in the number of particles of radius r due to their detachment from the particles with size $x > r$, and the second

term – the decrease in the number of particles due to separation of the particles with size $x < r$ from them.

Equation (4) is composed in such a way that for any mechanism of fragmentation the law of conservation of the total volume (and mass proportional to it) of particles in a solution is fulfilled:

$$\frac{\partial}{\partial t}\left(\int_0^\infty n(r,t)\frac{4\pi}{3}r^3\mathrm{d}r\right) = \int_0^\infty \frac{4\pi}{3}r^3\mathrm{d}r\frac{1}{r}\int_r^\infty B(x,r)n(x,t)\frac{\mathrm{d}x}{x^2}$$

$$-\int_0^\infty \frac{4\pi}{3}r^3\mathrm{d}r\frac{1}{r^5}\int_0^r B(r,x)n(r,t)x^2\mathrm{d}x = 0.$$

The function $B(x,r)$ determines the probability of formation of a particle of radius r from a particle of radius $x > r$ Assuming that fragmentation occurs according to the law (2), we set

$$B(x,r) = B_0\gamma(x)\left[\exp\left(-\frac{v(r)}{v_1}\right) + \left(-\frac{v(x)-v(r)}{v_1}\right)\right]\theta(r - r_{\min}). \quad (5)$$

This form of the function $B(x,r)$ is dictated by the following. Particles of small size (up to a monatomic) are most likely to be produced. The first term describes separation of small particles from the initial particle. The second term takes into account the fact that separation of a small particle of volume v from a large particle of volume V is simultaneously accompanied by the emergence of a particle of volume $V' = V - v$, close to V, in the system. The coefficient $\gamma(x) \approx (x/r_{10})^2$ takes into account the fact that the number of small particles, detached from the larger one, is proportional to its surface (r_{10} is the normalisation size). The unit function $\theta(r - r_{\min})$ entering into $B(x,r)$ formally takes into account the fact that the radius of the particles cannot be less than the radius of an atom (for gold $r_{\min} = 0.144$ nm).

The parameter v_1 in (5) depends on the temperature of the ablated particle and, consequently, on the radiation intensity. We estimate the characteristic values of temperature, the nanoparticles acquired under irradiation. Because the typical size of the particles in our experiments did not exceed 60 nm, i.e., much less than the depth of absorption of laser radiation in gold, we can assume that the temperature is almost the same throughout its volume. The equation describing the heating of a single particle is given by

$$mc\frac{\partial T}{\partial t} = PA - P_{\mathrm{loss}}(T), \quad (6)$$

where m, c and T are respectively the mass, specific heat and temperature of the particle; $P = \pi R^2 I$ is the power of radiation incident on the particle; I is the intensity; R is the radius of the particle; A is the absorbance of the particle; P_{loss} is the heat loss power. Assuming that the time for establishing thermal equilibrium is small compared with the duration of the pulse, we can take

$$PA = P_{\mathrm{loss}}. \quad (7)$$

To find P_{loss}, we will write in a quasi-stationary approximation the equation for the temperature distribution in the liquid surrounding the particle:

$$\frac{1}{r^2}\frac{\partial}{\partial r}\left(\kappa(T)r^2\frac{\partial T}{\partial r}\right) = 0, \quad r > R, \quad (8)$$

$$T|_{r\to\infty} \to T_0.$$

According to the tabulated data given in [9, 10], at temperatures $T \sim 10^3$ K and densities $\rho \sim 1$ g cm^{-3} the thermal conductivity of water depends on temperature according to the law

$$\kappa(T) \approx \kappa_0\left(\frac{T_0}{T}\right)^\beta, \quad (9)$$

where the parameter $\beta \approx 1.1$. For estimates we assume $\beta = 1$. Then from (8) we find

$$T = T_0\exp(-a/r). \quad (10)$$

Knowing the temperature distribution of the liquid in the vicinity of the particle size, P_{loss} can be found from the formula

$$P_{loss} = -4\pi R^2\kappa(T)\frac{\partial T}{\partial r}\Big|_{r=R}. \quad (11)$$

Taking into account (10) and (7), we obtain $a = (4\pi\kappa_0 T_0)^{-1}P_{\mathrm{loss}}$ and

$$T = T_0\exp\left(\frac{PA}{4\pi\kappa_0 T_0}\frac{1}{r}\right). \quad (12)$$

In particular, when $r = R$, we find the temperature of the particle:

$$T = T_0\exp\left(\frac{PA}{4\pi\kappa_0 T_0}\frac{1}{R}\right). \quad (13)$$

In the case of nanoparticles, when $kR \ll 1$ ($k = 2\pi/\lambda$ is the wave number), the absorbance A, according to the Mie theory, is given by

$$A = \frac{8\pi R}{\lambda}\mathrm{Im}\left(\frac{\varepsilon - \varepsilon_0}{\varepsilon + 2\varepsilon_0}\right), \quad (14)$$

where ε and ε_0 are respectively the dielectric constants of the particle and the medium surrounding the particle. Because $P = \pi R^2 I$, we finally obtain

$$T = T_0\exp\left(\frac{R^2}{R_0^2}\right), \quad R_0^2 = \frac{\kappa_0 T_0\lambda}{2\pi I}\frac{1}{\mathrm{Im}[(\varepsilon - \varepsilon_0)/(\varepsilon + 2\varepsilon_0)]}. \quad (15)$$

For gold (a bulk sample) at $\lambda = 0.5$ μm the dielectric constant is $\varepsilon = 3.91 + 2.04$i. Accordingly, the factor $\xi(\varepsilon_0) = \mathrm{Im}[(\varepsilon - \varepsilon_0)/(\varepsilon + 2\varepsilon_0)]$ is of order of unity. In particular, for water $\xi(1.33) = 1.42$.

For the parameters

$$\lambda = 0.51\ \mu\mathrm{m},\ \kappa_0 = 0.6\ \mathrm{W\ m^{-1}\ K^{-1}},\ T_0 = 300\ \mathrm{K},$$

$$I = 2\times 10^7\ \mathrm{W\ cm^{-2}} \quad (16)$$

we find for $\xi(\varepsilon_0) = 1.42$

$$R_0^2 = 51.4\ \mathrm{nm}^2,\quad R_0 = 7.2\ \mathrm{nm}. \quad (17)$$

As mentioned above, at a laser wavelength of $\lambda \approx 0.5$ μm plasmon resonance is observed for the gold nanoparticles. Consequently, the scale factor R_0 decreases. As a result, the heating efficiency of the particles and the fragmentation probability increase.

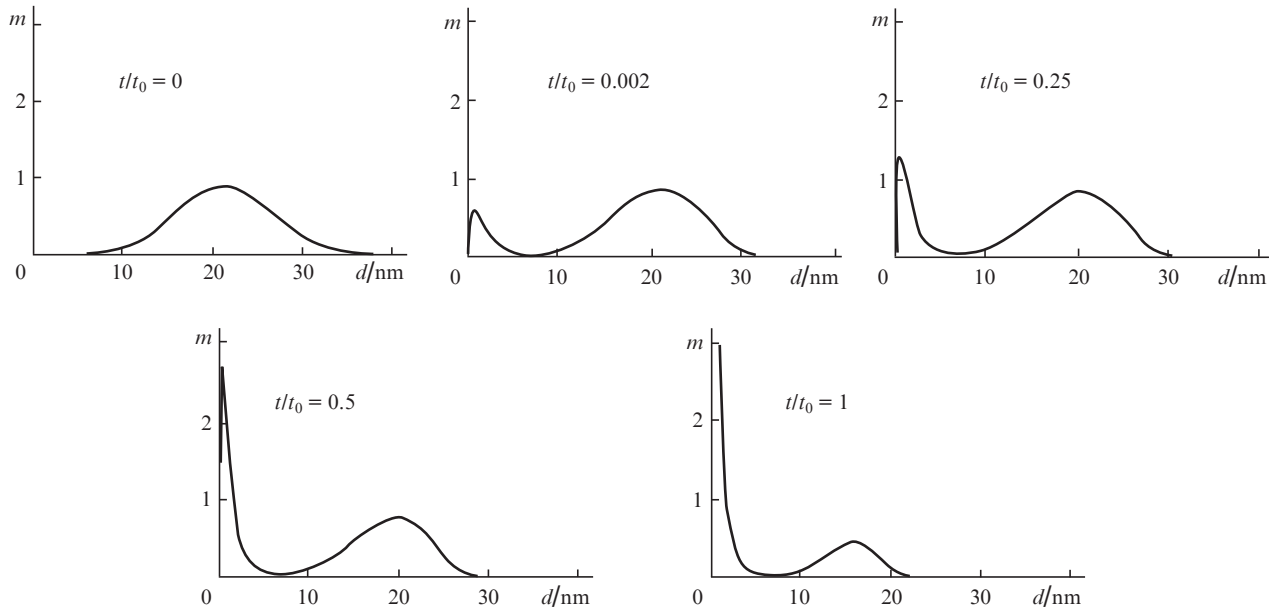

Figure 5. Nanoparticle diameter distribution functions $m(d)$ at different instants t/t_0, obtained by numerical solution of kinetic equation (7).

Note also that the limit of applicability of (14) corresponds to $R \sim 40$ nm, since the Mie theory is valid only if $kR < 1$. For 510-nm radiation used in our experiments, this corresponds to the specified size range. Therefore, in the calculations given below we used the interpolation expression

$$A(R) = \frac{A_{\text{Mie}}}{1 + R/R_{\text{M}}}, \qquad R_M = \frac{A_\infty}{A_{\text{Mie}}} = \frac{A_\infty}{8\pi\lambda\,\text{Im}[(\varepsilon - \varepsilon_0)/(\varepsilon + 2\varepsilon_0)]}, \tag{18}$$

where A_∞ is the absorbance of a bulk sample of gold, which is almost independent of its size. This formula is consistent with the theoretical calculations given, for example, in [11, 12].

Assuming that the rate of fragmentation of the nanoparticles is determined by temperature, as in the ordinary law of evaporation, we set in equation (5)

$$v_1 = v_{10}(T/T_0). \tag{19}$$

In solving the kinetic equation (4) we assumed that the temperature dependence of the particle size is given by the evaluation formula (15), which can be represented as

$$T = T_0 \exp\left(\frac{\alpha R^2}{1 + R/R_{\text{M}}}\right). \tag{20}$$

In this case, the numerical value of R_{M} was assumed equal to 40 nm. According to (15), the parameter α is proportional to the radiation intensity.

Thus, the constructed model (4), (5), (19) (20) contains actually one numerical parameter v_{10}, which is not defined theoretically. In numerical calculations we assumed $r_{10} = 0.05$ nm, $v_{10} = 4\pi r_{10}^3/3 = 5.2 \times 10^{-4}$ nm^3. The exact value of the coefficient B_0 is not essential, because it only determines the time scale of evolution of the distribution function and can be obtained by comparing the theoretical and experimental results.

The results of the numerical solution of the kinetic equation for the mass and diameter distribution function of particles $m(d)$ are shown in Fig. 5. Time is indicated in relative units t/t_0. In these units, the process duration was limited by the time $t/t_0 = 1$. It is assumed in this case that $B_0 = 0.5 \times 10^4$. The distribution functions are presented for five consecutive points in time: $t/t_0 = 0$, 0.002, 0.25, 0.5 and 1. The calculations are performed for $\alpha = 0.015$. Note that this value, in accordance with the formula (15), corresponds to the intensity of 2×10^7 W cm^{-2}. The values of other parameters are listed above.

One can see from the graphs that there is a gradual decrease in the number of large particles and an increase in small particles, and as a result, a new maximum in the distribution function is formed. Then, due to fragmentation of small particles there appear subnanometre particles, forming a colloidal solution of gold. This stage is slower than the previous one due to a decrease in the rate of fragmentation with decreasing particle size.

Figure 6 shows the distribution functions obtained in the numerical calculation for different values of the radiation intensity (parameter α).

5. Conclusions

We have studied the dynamics of fragmentation of nanoparticles in a colloidal solution under the action of laser radiation. Comparison of theoretical results (Figs 5 and 6) with the experimental results (Figs 2 and 3) shows that the assumptions made in constructing the model are justified, and the simulation results are in good agreement with experimental data.

The constructed model does not account for certain factors. In particular, we have not considered the dynamics of a vapour-gas layer in the vicinity of nanoparticles, which affects the temperature variation of the particle during each pulse. In addition, the model does not take into account the shift of the plasmon resonance of nanoparticles during their melting and formation of a vapour-gas shell around them [13].

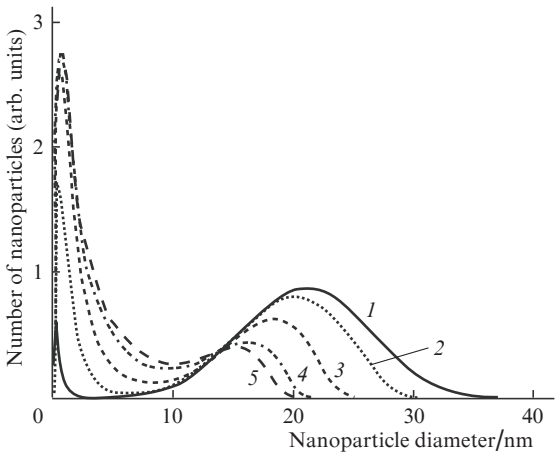

Figure 6. Nanoparticle diameter distribution functions at different values of the parameter α (intensity): 0.01 (*1*), 0.015 (*2*), 0.02 (*3*), 0.025 (*4*) and 0.0275 (*5*).

An important result of the paper is the conclusion that ablation of metal and fragmentation of the nanoparticles in vacuum (or a gaseous medium) differs much from ablation in a liquid. In particular, if ablation in vacuum is accompanied, as a rule, by formation of subnanometre-size particles (including monatomic particles), not only small particles, but also, with a high probability, relatively large fragments are produced in a liquid. Our calculations show that fragmentation of nanoparticles via their halving, anticipated in earlier work [8], is not realised.

The simulation results well describe the changes in the distribution function of silver nanoparticles in water upon their fragmentation by femtosecond laser radiation, experimentally investigated in [5]. We have also observed the appearance of the second peak of the distribution function in the region of small sizes, although the initial size of the nanoparticles differed significantly from the size of particles that are the subject of this research work, and exceeded 100 nm.

References

1. Sibbald M.S., Chumanov G., Cotton T.M. *J. Phys. Chem.*, **100**, 4672 (1996).
2. Procházka M., Mojzeš P., Štepánek J., Vléková B., Turpin P.-Y. *Anal. Chem.*, **69**, 5103 (1997).
3. Mafuné F., Kohno J.-Y., Takeda Y., Kondow T., Sawabe H. *J. Phys. Chem.*, **B105**, 5144 (2001).
4. Tsuji T., Iryo K., Watanabe N., Tsuji M. *Appl. Surf. Sci.*, **202**, 80 (2002).
5. Akman E., Genc Oztoprak B., Gunes M., Kacar E., Demir A. *Photonics and Nanostructures – Fundamentals and Applications*, **9**, 276 (2011).
6. Shafeev G.A., Freysz E., Verduraz F.B. *Appl. Phys. A*, **78**, 307 (2004).
7. Boson-Verduraz F., Brayner R., Voronov V.V., Kirichenko N.A., Simakin A.V., Shafeev G.A. *Kvantovaya Elektron.*, **33** (8), 714 (2003) [*Quantum Electron.*, **33** (8), 714 (2003)].
8. Simakin A.V., Voronov V.V., Kirichenko N.A., Shafeev G.A. *Appl. Phys. A*, **79** (4–6), 1127 (2004).
9. Pustovalov V.K. *Chem. Phys.*, **308**, 103 (2005).
10. Grigoriev I.S., Meilikhov E.Z. (Eds) *Handbook of Physical Quantities* (Boca Raton, NY, London: CRC Press, 1996; Moscow: Energoatomizdat, 1991).
11. Link S., El-Sayed M.A. *J. Phys. Chem. B*, **103**, 4212(1999).
12. Link S., El-Sayed M.A. *Int. Rev. Phys. Chem.*, **19**, 409 (2000).
13. Siems A., Weber S., Boneberg J., Plech A. *New J. Phys.*, **13**, 043018 (2011).